JOURNAL OF MATERIALS SCIENCE **38** (2003) 4461 – 4470

Microrheology as a tool for high-throughput screening

V. BREEDVELD*,‡, D. J. PINE
Department of Chemical Engineering & Materials Research Laboratory, University of California, Santa Barbara, CA 93106-5080, USA
E-mail: victor.breedveld@chbe.gatech.edu

Microrheology can be used for high-throughput screening of the rheological properties of sample libraries of complex fluids. Two passive techniques are particularly suitable: video microscopy and diffusing-wave spectroscopy. The techniques complement each other very well and can be applied to samples that offer different experimental challenges. We offer a thorough analysis of the strengths and limitations of microrheology with the emphasis on high-throughput applications. To illustrate the potential of microrheology, results are presented for two representative cases: the rheological screening of aqueous solutions of a block copolypeptide library and the rheological phase diagram of a water/surfactant/salt system.

1. Introduction

Parallel and combinatorial chemistry have opened new pathways for the synthesis of large libraries of novel materials. Such approaches are particularly useful for polymers, whose properties can be tailored to meet specific requirements by manipulating their many degrees of freedom: molecular weight, backbone monomer, degree of branching or cross linking, and side group composition (partially or fully functionalized). In the case of copolymers, the number of possible architectures increases even further because of the virtually unlimited number of monomer combinations and relative compositions. With such an extended parameter space, combinatorial characterization techniques become useful because they can significantly accelerate and extend the systematic investigation of material properties.

In this paper, we explore the use of microrheology as a tool for high-throughput screening of large libraries of polymer melts and solutions. Conventional (macro) rheology has proven to be an important method for studying the mechanical properties of polymer melts and solutions. Key quantities for characterizing their structure, strength, and processibility include the strain-rate dependent steady-state shear viscosity and the frequency dependent viscoelastic moduli. The classic technique for determining these quantities, mechanical rheometry, is slow and laborious. Loading a sample, performing measurements, and the subsequent cleaning of the rheometer limit the typical number of samples that can be characterized to 5–10 per day. By contrast, the high-throughput techniques described in this paper can be one or two orders of magnitude faster, thus making them ideal for characterizing the vast libraries that need to be screened. This screening might be used to locate phase boundaries for structural transitions, for gelation, or to differentiate samples according mechanical or rheological properties. The key points are that only a small amount of each sample is required and that each rheological measurement can be automated and performed quickly.

In Section 2 the concept of microrheology is explained and a review of the work in this field is provided in order to set the stage for its application as a high-throughput screening method. Section 3 describes two complementary implementations of microrheology, both suitable for a combinatorial approach. In the final two sections we provide some practical guidelines for using microrheology as a rapid screening tool and illustrate the method with measurements from our laboratory.

2. Microrheology

True to its name, microrheology is best described as "rheology on the micrometer length scale." It involves using microscopic mechanical probe particles to measure the relation between stress and deformation in materials. Analogous to macroscopic mechanical rheometry, a known stress (probe force) is applied by the probe particle and the resulting deformation (probe position) is measured. From these quantities the rheological properties of the medium can be derived. As a result of the miniaturization, microrheology typically requires less than 10 *micro*liters of sample, while a traditional mechanical rheometer requires at least a few *milli*liters. The dramatic decrease in sample volume makes it feasible to perform rheological measurements in situations where only a limited amount of material is available, e.g., biological samples. For cases of large libraries for high-throughput screening, the reduced

*Author to whom all correspondence should be addressed.
‡*Current address*: School of Chemical and Biomolecular Engineering, Georgia Institute of Technology, Atlanta, GA 30332-0100, USA.

sample size has an additional advantage: it relieves the synthetic chemist from the burden of producing materials on the gram scale.

The concept of using microscopic probe particles to measure mechanical properties dates back to the early twentieth century, when magnetic particles were embedded to study the elasticity of gelatin gels [1]. Over the last decade rapid developments have occurred in the field (for recent reviews, see e.g., [2–4]). Technological innovations in light scattering and video microscopy, as well as theoretical advances have renewed interest in and greatly expanded the power of microrheology. Current techniques can be divided into two main categories: *active* methods that involve probe manipulation and *passive* methods that rely on thermal fluctuations to induce motion of the probes. In this paper we focus mainly on passive methods, but provide a short overview of active methods and their specific properties since for certain specific applications these can be favorable.

2.1. Active methods

The earliest experimental implementation of microrheology was based on the manipulation of magnetic beads with an external magnetic field [1]. Because of limited control over the forces, non-sphericity of particles and inaccuracy of the detected particle position, these measurements only provided qualitative rheological data. Modern versions have improved accuracy and are capable of quantitative rheological characterization of the embedding medium under the application of constant or oscillatory forces, which respectively yield steady-shear viscosity and viscoelastic moduli [5, 6]. The rheological properties of many interesting systems, including the cytoplasm of living cells [7], have been measured in this way.

A modern alternative to magnetic manipulation of small particles is the use of optical tweezers. The electric field gradients of a highly focused laser beam result in a local trapping force that pulls the particle towards the waist of the focused beam [8]. High-aperture objectives on an optical microscope can be used conveniently to simultaneously trap and image the probe particle [9]. The local trapping force can be calibrated. Then, by moving the beam and observing the particle response, the local rheological properties of the embedding medium can be determined. The main advantage of optical tweezers over magnetic methods is the localization of the applied force.

A third method for applying sample deformation on microscopic length scales is atomic force microscopy (AFM). The technique is widely used to image surfaces with atomic resolution, but the nanometer position-control and sensitivity as a force transducer make AFM a logical choice for rheological measurements as well [10, 11]. The cantilever tip is used to indent the surface of a sample and sinusoidal modulations are superimposed to measure frequency dependent mechanical responses that can be interpreted in terms of elastic and viscous dynamic moduli. The AFM technique is capable of generating larger stresses (0.1–10 kPa) than the other two methods and in combination with the imaging capability it is particularly useful for the characterization of thin samples, e.g., films, coatings and cell surfaces. Because it is inherently a surface method, the results are sometimes difficult to translate into bulk properties.

2.2. Passive methods

Instead of using an external excitation to move the probe particles, the intrinsic Brownian motion of the particles can be used. In this case, the driving force is thermal, with a known energy scale corresponding to $k_B T$. An advantage of this approach is that no external driving force is required, i.e., the method is passive. Because the thermal driving force is small, no sample deformations occur that exceed equilibrium thermal fluctuations. This virtually guarantees that only the linear viscoelastic response of the embedding medium is probed. Active methods, by contrast, can easily rupture weak structures. While it may be advantageous to have access to non-linear steady shear viscosity in some cases, it also means that an amplitude sweep must be performed for every sample to confirm linearity, similar to macroscopic rheometry.

One drawback of using Brownian motion as the driving force is that thermal energy is fixed and limited to $k_B T$, so that the stress will be sufficiently large to generate detectable particle motion only in relatively soft materials, such as polymer solutions and gels. Measurements in polymer melts and solids are much more difficult. Nevertheless, with modern detection techniques spatial resolutions ranging from 0.1 to 10 nm can be achieved, so that microrheology measurements can be performed on many complex fluids. In Section 4 quantitative estimates of the limits of operation are provided.

An intuitive theoretical basis for passive microrheology is provided by considering two extremes: a particle with radius a that is embedded in a purely viscous Newtonian liquid or a fully elastic network. In case of a Newtonian liquid with viscosity η the particle motion is diffusive with a diffusion coefficient given by the Stokes-Einstein relation $D = k_B T/6\pi\eta a$. For diffusive motion, the d-dimensional mean-squared displacement (MSD) is given by

$$\langle \Delta \mathbf{r}^2(\tau) \rangle \equiv \langle |\mathbf{r}(t+\tau) - \mathbf{r}(t)|^2 \rangle = \frac{d\, k_B T}{3\pi\eta a}\tau \qquad (1)$$

where the brackets denote averaging over all starting times t and τ is the lag time. The Stokes-Einstein relation enables viscosity measurements by observing the time-dependent MSD of a particle of known size.

If the same particle is embedded in a purely elastic medium with a storage modulus G, there will be a maximum to the displacement $\Delta\mathbf{r}$, occurring when the thermal energy $k_B T$ of the particle equals the elastic energy associated with the deformed network. In terms of the MSD this means that a plateau is reached for long lag times:

$$\langle \Delta \mathbf{r}^2 \rangle_{\tau\to\infty} = \frac{d\, k_B T}{3\pi G a} \qquad (2)$$

Most materials, however, exhibit more complex behavior with a frequency dependent viscoelastic response that has both viscous and elastic components. These materials are characterized by the complex modulus $G^*(\omega) = G'(\omega) + iG''(\omega)$ that is usually measured with oscillatory mechanical rheometry. For these cases a generalized Stokes-Einstein relation (GSER) has been formulated, which is a natural extension of Equations 1 and 2 to the Laplace frequency domain [12]. In this case, a frequency dependent MSD is obtained:

$$\langle \Delta \tilde{r}^2(s) \rangle = \frac{d\, k_B T}{3\pi a s \tilde{G}(s)} \tag{3}$$

where s is the Laplace frequency. The two moduli $G'(\omega)$ and $G''(\omega)$, which respectively represent the elastic and viscous response of the material, can be determined from the single real function $\tilde{G}(s)$, since they are related to each other through the Kramers-Kronig relations. The derivation of Equation 3 has been the seminal breakthrough for passive microrheology. Although originally derived on a rather *ad hoc* basis, the GSER has since been shown to be an extremely valuable tool with a strong theoretical backing [13]. Direct comparison with macroscopic rheological data has revealed excellent agreement, often beyond limits where it might be anticipated.

The range of frequencies over which Equation 3 is valid is limited by two effects: inertia and compressibility [13, 14]. At very high frequencies the penetration depth of the deformation waves caused by the probe particle in the surrounding liquid becomes comparable to the probe size. In a mechanical rheometer this effect usually comes into play between 10 and 100 Hz for low-viscosity fluids, because the relevant length scale is the gap size, typically about 1 mm. The smaller size of the microscopic probe delays the onset of this effect into the MHz-regime for microrheology, thus opening a new window of timescales. At the low frequency end of the spectrum, there is a concern about the compressibility of the viscoelastic medium, which generally consists of an elastic network surrounded by an incompressible fluid. Consider, for example, polymer chains in solution or a polymer gel. At low deformation rates, the motion of network and liquid can decouple and the liquid drains freely through the network. The medium then no longer responds as a continuum and the assumptions on which Equation 3 is based break down.

The use of the GSER reduces the practical task for the experimentalist to the determination of the time-dependent MSD. The techniques that have been employed to achieve this can be divided into three classes: single-particle laser detection [14, 15], ensemble averaged light-scattering [12, 16] and video microscopy [17, 18]. The latter two will be discussed in more detail in Section 3, since they are most suitable for high-throughput applications.

The main characteristics that distinguish between the methods are the accessible frequency range and spatial resolution. Single-particle laser detection uses a set-up similar to optical tweezers and tracks the motion of a single particle over time. It has single particle resolution and a large potential frequency range, up to the MHz regime. Scattering techniques have lower spatial resolution, since they average the MSD over multiple particles, but they span a similarly large frequency domain (well into the MHz range). Scattering techniques also allow for more rapid data acquisition because of the inherent ensemble averaging that takes place during light-scattering. Video microscopy is limited by the video capture rate, which is 60 Hz for a standard NTSC video system, but can be faster using specialized cameras. Many particles can be captured in the field of view (ca. 100). This provides a great deal of flexibility: for homogenous systems averaging over all particles improves the statistics of the MSD; in case of spatial heterogeneity one can actually verify and quantify variations in local rheology over the observed sample volume [10, 19].

Once the MSD has been found the real challenge is over. Various computational schemes can be employed to extract the dynamic moduli $G'(\omega)$ and $G''(\omega)$, but all the crucial information is available in the MSD. When plotted as a function of time on a double logarithmic plot, the slope of the graph $\langle \Delta \mathbf{r}^2(\tau) \rangle \sim \tau^\alpha$ must fall between the viscous ($\alpha = 1$) and elastic ($\alpha = 0$) extremes (Equations 1 and 2). Deviations of the slope α from these integer values are indicative of viscoelastic relaxation processes in the medium (see Fig. 1). In

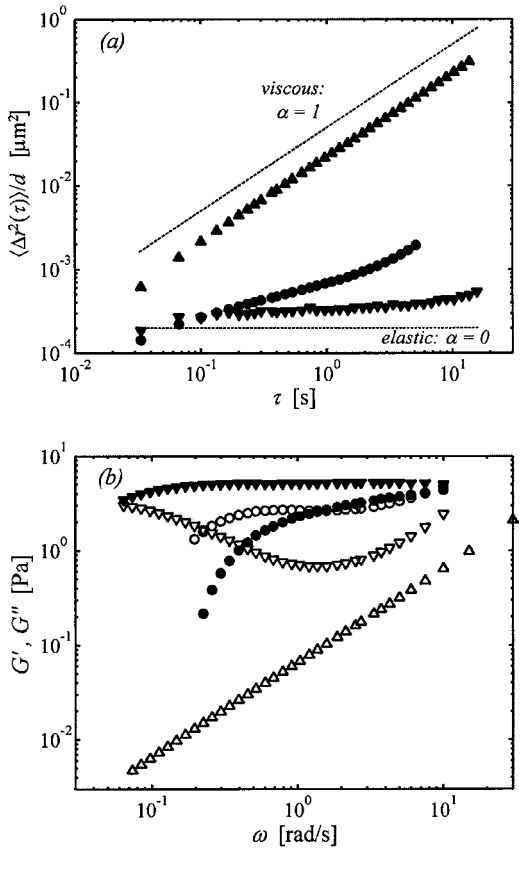

Figure 1 (a) Mean-squared displacement as a function of lag time for Newtonian (▲, water-glycerol mixture), mostly elastic (▼, $K_{160}L_{40}$ gel at 0.25 wt% polymer) and viscoelastic (●, K_{160} (rac-L)$_{40}$ solution at 2.0 wt%) fluids (see Section 5.1 and [20] for diblock copolypeptide information); MSD's are normalized by the dimensionality d. (b) Corresponding dynamic moduli G' (closed symbols) and G'' (open), calculated using Equation 3 with the second-order logarithmic polynomial fit [21]. Data was measured with amidine-functionalized polystyrene spheres with diameter $a = 0.53$ μm and 100× objective.

many cases, conclusions about sample rheology can be drawn directly from the MSD. Often it is not necessary calculate dynamic moduli. If it is somehow desirable, Equation 3 provides the recipe, but practical issues arise when performing (inverse) Laplace and Fourier transforms to a discrete data set over a limited frequency domain. Especially near the edges of the domain, significant errors can occur due to the numerical implementation of the transformations. Instead of the direct route [14] an alternative approach is to locally fit the MSD $\langle \Delta \mathbf{r}^2(\tau) \rangle$ to a first- or second-order logarithmic polynomial after which $G^*(\omega)$ can be calculated algebraically [21, 22]. These schemes have proven to be robust within an accuracy that is acceptable for rheology, with a maximum 5–10% error for simulated noise-free data.

2.3. Heterogeneous samples

In deriving the equations above it has been assumed that the embedding medium is homogenous on a length scale comparable to the size of the probe particles. Under this condition the probe particles sample the macroscopic bulk rheological properties of the medium during their thermal motion. By contrast, if the system possesses structures with characteristic lengths scales comparable to the size of the probe particles, the assumptions of homogeneity on which Equation 3 are based are not valid. In some cases, the mere presence of the probe particle can lead to changes in the local environment surrounding the particle, e.g., through adsorption or depletion, so that a straightforward application of Equation 3 leads to systematic errors.

An important quantity for assessing potential problems in using Equation 3 is the typical size ξ of the structural elements that constitute the viscoelastic medium. For polymer networks this should be the mesh size, in emulsions the droplet size, in porous systems the pore size, etc. As long as ξ is much smaller than the particle radius a, it is usually safe to apply the GSER and interpret the microrheological measurements as reflecting bulk properties. Comparison of length scales is not always sufficient. Often the dynamics play a role as well. In mixtures of colloidal rods it was found [23] that the diffusion coefficient of added tracer spheres is governed by the macroscopic viscosity (Equation 1) and does not depend on rod size as long as the rods are relatively mobile. Only at high concentrations, when the rods get entangled and immobilized, size does matter: in this case tracer spheres must be larger than the pores to obey the Stokes-Einstein relation. Another striking example was the initial work on microrheology of concentrated emulsions, where the emulsion droplets act as tracers themselves [12]. Although $\xi \sim a$, microrheology was in excellent agreement with bulk measurements.

Since the interaction of embedded probe particles with the medium strongly depends on the system under investigation, it is impossible to provide a general recipe for successful measurements. For each new complex fluid the choice of probe particles needs to be addressed carefully, as will be illustrated in Section 4.2. A very pragmatic way to deal with this is to prepare samples with different probes, varying size and surface chemistry. Robustness of the results against such changes supports reliability. If sample material is available in sufficient quantity, a some macroscopic rheological experiments can also be performed to benchmark the results.

Recently, a so-called two-particle microrheology method has been developed to extract bulk rheology from microscopic measurements in heterogeneous samples [13, 18]. The idea was to rely on hydrodynamic interparticle interactions and measure how one particle's motion is correlated with that of another. To this purpose the two-particle *cross*-correlation of the particles' displacement is measured instead of the *auto*-correlation of single-particle displacement. The cross-correlation function is a direct measure of the strain field generated by the Brownian tracers *between* the particles, that is, on interparticle length scales of typically 10–100 μm rather than the particle size length scale of approximately 1 μm.

Realizing that the motion of particles in an incompressible medium is coupled by hydrodynamic interactions that decay as $1/r$ for $r \gg a$ (r being the interparticle distance), the cross-correlation of particle displacements can directly be related to the rheology of the medium, averaged over the interparticle distance r:

$$\langle \Delta \tilde{r}_\mathrm{i}(r,s) \Delta \tilde{r}_\mathrm{j}(r,s) \rangle_{i \neq j} = \frac{k_\mathrm{B} T}{2\pi r s \tilde{G}(s)} \qquad (4)$$

where Δr_i and Δr_j are the displacements of two particles i and j along their center-to-center vector. Averaging over this larger length scale dramatically reduces the sensitivity to changes in the immediate surroundings of the probes. As an added bonus, particle size and shape drop out of the equation: particles are treated as point sources in the deformation field. Therefore even polydisperse probe particles can be used. The main disadvantage of two-particle microrheology is the fact that calculating cross-correlation functions requires significantly more data and is computationally more intensive than determining auto-correlation functions. Because of this constraint, video microscopy is currently the most suitable technique, since it simultaneously tracks the motion of up to a few hundred particles. By combining one- and two-particle analysis heterogeneity can in principle be detected in the sample without the need of additional experiments.

3. High-throughput rheology

Rheological properties often change by many orders of magnitude when a phase boundary is crossed or when other structural changes like gelation occur. This makes rheology a suitable candidate not only for screening mechanical properties, but also for mapping out other phenomena that are directly correlated with rheology, such as phase behavior and gelation. Having introduced the general concept of microrheology, in this section we discuss how it can be applied as a high-throughput method.

The implementation of microrheology for screening purposes imposes certain specific demands. First of all,

any suitable technique must offer significant speed advantages over conventional rheology in order to handle large numbers of samples. Additionally, the method of choice should be capable of dealing with large variations in material properties without intervention from the operator. Systematical detection of such variations is after all the goal of high-throughput screening.

Two complementary techniques that satisfy these requirements of speed and robustness are video microscopy and diffusing-wave spectroscopy (DWS), which are described below.

3.1. Video microscopy

Video microscopy [17, 18] is probably the simplest and most intuitive of all microrheology implementations. The motion of Brownian probe particles is monitored under an optical microscope, either in bright-field or fluorescent mode depending on the nature of the tracer particles. In order to obtain the mean-squared displacement, movies are recorded with a CCD camera. Subsequently, the tracer particle positions are analyzed in each frame of the movie. Finally, these positions are linked to identify the trajectories of individual particles.

Initial versions of the technique captured the output of an analog CCD camera (30 Hz frame rate, 640×480 pixels) on video tape. The desired parts of the tape were then digitized with a frame grabber on a PC. Ever increasing computer speed and memory now enable direct capture of the CCD video output onto computer hard disk by means of dedicated software developed in the Sackmann group (OpenBox [24]). Image analysis routines for particle detection and tracking, based on the original work of Crocker and Grier [25], have been further developed in the Weitz group (e.g., [18]). The procedures are available as freeware in the form of macros for the software package IDL (Research Systems Inc, Boulder, CO).

The spatial resolution of video microscopy is determined by optical magnification and CCD pixel density. In our lab, a $100\times$ oil-immersion objective on a Nikon inverted microscope in combination with a 640×480 pixel CCD camera (Cohu, Poway, CA) on the photo port leads to a resolution of 0.129 μm per pixel. Even thought this resolution is beyond the diffraction limit (ca. 250 nm for visible light on a high quality microscope), the particle position can be determined with even greater precision, to subpixel accuracy. As long as the particle diffraction image is spread over 5–10 CCD pixels, one can fit the observed intensity profile to a Gaussian distribution. If the proper settings are used, the particle position can be found with 0.1 pixel accuracy. Of course, optical measurements of the particle size are still limited by diffraction, but the position of a single particle can be determined with subpixel accuracy so long as the density of particles is sufficiently low that particle images do not overlap. Subpixel resolution is only meaningful if the shutter speed of the camera is short enough to prevent significant particle motion during the generation of each image.

Temporal resolution of a standard CCD camera is limited to 1/60 s when the two fields that constitute each video frame are split and analyzed separately. Splitting the full image into two 640×240 images decreases the spatial resolution, especially in the vertical direction, since each particle covers fewer CCD pixels, but the temporal benefits are significant. The frequency range can be extended further by using high-speed video cameras.

In a typical measurement, there are 100 particles within the field of view. Under these circumstances 50 s of data acquisition (1500 images) is usually sufficient to obtain reliable statistics up to a lag time $\tau = 3$ s. Longer lag times require proportionally longer acquisition times. As a rule of thumb, the ensemble averaged MSD must consist of at least 500 independent contributions to provide a meaningful value. On a relatively modern PC (1.5 GHz, 512 Mb RAM) the image analysis and data processing of 1500 images (400 Mb) takes about 15 min, from movie to MSD.

In practice, the frequency domain of standard video-based microrheology is limited to two and a half decades even in the best possible scenario: 0.1 to 60 Hz. In comparison to other methods this is rather mediocre and for detailed quantitative rheological studies it is often insufficient, because relaxation processes typically span more than a decade in frequency.

Nevertheless, the benefits of the method are considerable. First of all, the set-up is simple and robust. The hardware consists of a research-grade inverted microscope, video camera and dedicated image analysis computer. Most of these are present in modern research labs. Secondly, the images are accessible to check the distribution of the tracers and make sure that no aggregation has taken place. Finally, the detailed knowledge about temporal and spatial distribution of single-particle tracks enables advanced statistical analysis to identify clusters of particles that have a similar microenvironment [19]. This approach has been used successful to study the local rheology of living cells with high spatial resolution [26]. The two-particle method described in Section 2.3 is also a natural tool to be applied to video microscopy data sets.

For high-throughput applications, a multi-sample set-up with automation is desirable. In the case of video microscopy the main issue that must be dealt with is efficient sample preparation. Multi-well plates with Nr. 1.5 cover glass optical bottoms are available commercially (Nalge Nunc International, Rochester, NY). The real challenge is to get samples into these 100–200 μl wells at the right composition and with the probe particles properly mixed in. In the next section we discuss the problems we encountered in some of our applications. Once the sample is in place, taking movies is a relatively fast and easy task. Although it can easily be automated with a computer controlled microscope stage, our experience is that for a 96-well plate manual acquisition of 50 s movies is relatively painless in comparison with sample preparation. The time-consuming step is the image analysis and data processing. As mentioned above, this still requires about 15 min per movie, but significant reductions are anticipated with the progress of computer development. The full analysis on all movies of a plate can easily

be performed automatically by means of a computer macro for IDL. All in all, measuring 96 samples currently requires about 24 h of computer time, 1.5–2 h of video recording and a highly system dependent amount of preparation time. Once the recording phase has been automated, the speed of the method is only limited by computational power, which is relatively cheap and guaranteed to improve in the near future.

3.2. Diffusing-wave spectroscopy

A complementary method to video microscopy is diffusing-wave spectroscopy (DWS) (see [27] for a thorough introduction to the subject and [28] for a recent review). The method was developed in the late 80's and has evolved into a powerful tool for investigating the dynamics of concentrated, highly scattering systems like emulsions, colloidal suspensions, and foams. The sample is illuminated with a laser beam; the key idea is that the laser light experiences a very large number of scattering events before exiting the sample. The outgoing light is collected in either the forward or backward scattering direction and projected onto a conventional dynamic light-scattering detection system consisting of photomultiplier tube, amplifier-discriminator and digital correlator (Fig. 2). Because the light is scattered from many particles, angular information is lost. However, each particle only needs to move over a small fraction of the wavelength to generate decorrelation of the light. The spatial resolution can thus reach the Angstrom level. The temporal resolution of the method is also extremely high, up to 10 MHz in an ordinary off-the-shelf system. The lower frequency limit depends on the desired signal-to-noise level, stability of the laser, and patience of the experimentalist, but is typically about 1 Hz.

The advantage of DWS is that ensemble-averaging takes place on the fly and the intensity correlation function can be directly transformed into a time-dependent MSD. The procedure requires application of the Siegert relation, careful calibration of the DWS set-up with a reference sample and straightforward numerical analysis [27]. This beats the time-consuming image analysis step of video microscopy. At the same time, however, the inherent ensemble averaging disables the advanced statistical treatment that is possible with single-particle trajectories. At about 1 vol% DWS requires a larger concentration of probe particles than video microscopy, where 0.02% usually suffices for spheres with 0.5 μm diameter.

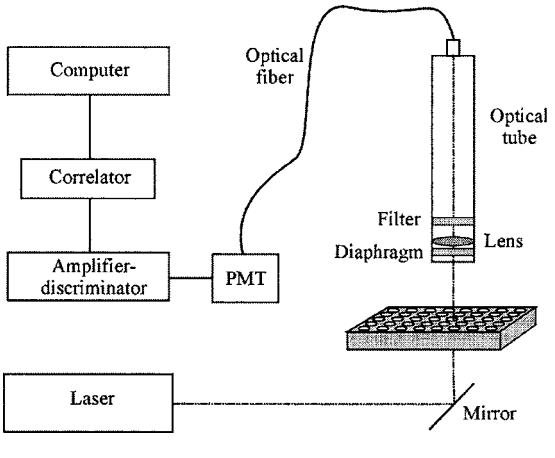

Figure 2 Diffusing-wave spectroscopy set-up for high-throughput screening. To facilitate the use of a multi-well plate, the laser beam is deflected upward and shines through the glass bottom. The speckle pattern on the free surface of the sample is imaged onto an optical fiber that connects to the photomultiplier tube. An optical tube with diaphragm, lens and optical bandpass filter is used to minimize stray light.

4. Practical considerations

4.1. Limits of operation

As briefly discussed in Section 2.2 the fixed amount of thermal energy associated with Brownian motion restricts the applicability of passive microrheology techniques. Fig. 3 presents some practical examples where the results are influenced by the operational limits.

The most important implication of the limited thermal energy available from Brownian motion is an effective upper limit to the viscosity and/or elasticity, since the tracer particle must diffuse over a distance that exceeds the detection resolution. Equations 1 and 2 can be used to estimate these limits

$$\eta_{\max} = \frac{d\, k_B T}{3\pi a \delta^2}\tau \qquad G_{\max} = \frac{d\, k_B T}{3\pi a \delta^2} \tag{5}$$

δ being the spatial resolution. For a viscous liquid the maximum viscosity depends on the lag time τ; in principle one can always wait long enough to see the mean-squared displacement rise above noise level. Also, decreasing the particle size shifts the limits, simply because smaller particles move faster with the same amount of energy. For viscoelastic liquids Equation 5 can be applied to estimate the upper boundary for the dominant dynamic modulus, G' or G''.

In our video based experiments ($d = 2$) we typically use particles with $a = 0.5$ μm together with a 60× objective and $a = 0.25$ μm with 100× magnification. Using the estimated 0.1 pixel resolution of $\delta = 22$ and 13 nm for the respective objectives results in $G_{\max} = 3.6$ and 21 Pa at ambient temperature. For a minimum lag time of 1 s, the same numerical values can

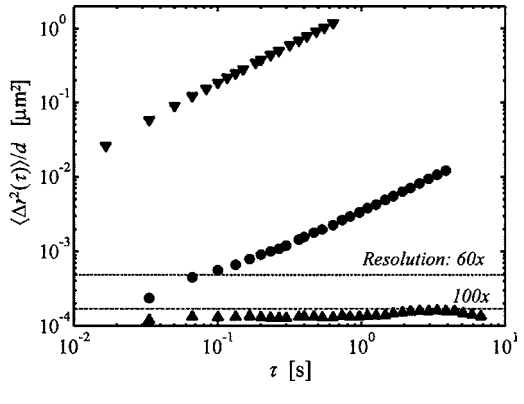

Figure 3 MSD as a function of lag time τ for 0.53 μm spheres (100× objective) in water (▼) where the fast motion limits the attainable lag times and for 1.1 μm beads (60×) in a highly viscous water-glycerol mixture (●) and a strong 4% gelatin gel (▲); in this case the spatial resolution of 22 nm for the 60× objective makes part of the data meaningless.

be used for η_{max} in a viscous system when expressed in Pa.s. Diffusing-wave spectroscopy ($d = 3$) has a better spatial resolution, $\delta \sim 2$ nm, so that with $a = 0.25$ μm the maximum elasticity improves to $G_{max} = 1300$ Pa. As a result of these limits, passive microrheology is only applicable to soft materials. Highly viscous polymer melts and very stiff gels are examples of systems that could be accessible with active probe manipulation. If the sample modulus becomes even higher, microrheological techniques can no longer be used.

In inviscid media, video microscopy has another operational limit: tracer diffusion can be so fast that the average tracer residence time in the field of view restricts the longest lag time for which the MSD can be measured. The maximum lag time can be estimated as:

$$\tau_{max} = \frac{3\pi a d_f^2 \eta}{2k_B T} \quad (6)$$

where d_f is the depth of focus, which depends on the microscope settings. Equation 6 shows that this is only relevant for small particles in low-viscosity media. For dilute aqueous solutions this results in an upper limit $\tau_{max} \sim 1$–2 s.

4.2. Probe particles

Colloidal tracer particles can be obtained commercially in a large variety of sizes, chemical compositions, and surface preparations. We have used particles from Interfacial Dynamics Corporation (Portland, OR) and Molecular Probes (Eugene, OR). Other sources are available, with Bangs Laboratories Inc. (Fishers, IN) being another of the large suppliers.

The most popular particles for microrheology experiments are polystyrene lattices. These particles have excellent sphericity and very low polydispersity. Their density (1.05 g/ml) is close enough to water to eliminate sedimentation over the course of the experiments. Polystyrene is hydrophobic, so the particles need to be stabilized against aggregation in an aqueous environment. The most commonly used method is charge stabilization with ionic surface groups. We have used sulfonated and carboxylated spheres with negative surface charge and positively charged particles with amidine surface groups. These lattices are stable at reasonably high salt concentrations, although the presence of multivalent counterions should be avoided as much as possible. If the system under investigation is highly charge sensitive and both positive and negative particles affect the rheological properties, alternatives such as sterically stabilized silica particles can be used.

Probe selection is one of the most important experimental choices to be made, since microrheology relies on the absence of interaction between embedding medium and probe particle. In some cases, basic knowledge of the experimental system is sufficient. When studying the microrheology of positively charged lysine-based block copolymers, it was hardly a surprise to find that positively charged polystyrene particles worked much better than negative ones, which aggregated under the presence of the polyelectrolyte. In many other cases, however, the choice is less obvious and the preparation of a few test samples with different particle types is advisable.

4.3. Sample handling and preparation

The preparation of sample arrays for high-throughput screening is often a challenge that rivals the actual experiments. In a 96-well plate the sample volume varies between 50 and 200 μl and in a 384-well plate the working volume is reduced even further to 10–50 μl. In principle, even less volume is needed, as little as 1 μl for video microscopy, but the presence of a free surface in multi-well plates imposes the need of a relatively large sample thickness to prevent surface effects.

One of the systems that we have studied is amphiphilic diblock copolypeptides in aqueous solution [20] (see Section 5.1). In our first attempts, a 6×4 array was synthesized were the total molecular weight was changed along one axis and relative block composition along the other. The most interesting rheological feature of these diblock copolypeptides is gelation, requiring that the rheology thus should be studied as a function of polypeptide concentration as well. In a 96-well plate, this means that each of the 24 block copolypeptides could be measured at four different concentrations: 0.1%, 0.3%, 1% and 3% by weight.

Getting the correct polypeptide concentrations into each well in a time-efficient and accurate manner is a non-trivial task. The most efficient route would be to prepare one stock solution for each polypeptide and dilute it with deionized water in the corresponding 4 wells to get the desired concentration series. However, like most complex fluids, polypeptide solutions are difficult to load and dispense quantitatively with a pipetter, because of their viscoelasticity. The elaborate route is to prepare each of the 96 samples outside the plates at the correct concentration in individual vials, by weighing and diluting the stock solution and adding the probe particles. Of course this approach takes away part of the elegance of combinatorial methods. As an intermediate solution, we used added salt (NaCl) to break down the gel in the 24 stock solutions of the individual polypeptides. Using a pipetter, known quantities of solution were transferred to each of the 96 wells. Then the plate was dialyzed against deionized water for several days and freeze dried. Finally, water and tracer particles were added to redissolve the copolypeptides at the desired concentration. This protocol involved two time-consuming steps, dialysis and freeze-drying, but requires relatively little human intervention.

Mixing small volumes of viscoelastic sample with tracer particles is an additional difficulty that should not be underestimated. It can be difficult to induce the necessary convective flow, even in low-viscosity fluids because the Reynolds number is small due to the sample size.

5. Applications

5.1. Gelation in block copolypeptide solutions

The high-throughput screening approach was succesfully applied to aqueous solutions of diblock

copolypeptides. These short polypeptide amphiphiles consist of a hydrophilic polyelectrolyte block and a shorter hydrophobic block. The copolypeptides are capable of forming hydrogels at remarkably low concentrations [20]. The gelation properties strongly depend on the molecular architecture: total molecular weight, relative block lengths and choice of hydrophobic peptide monomer all play an important role. The synthesis chemistry is flexible [29], yields monodisperse polypeptides and can handle a large variety of amino acid monomers. With the added potential to expand to multiblock designs, block copolypeptides are an excellent testcase for high-troughput rheology.

As noted in Section 4.3, our collaborators synthesized one library of poly-(L-lysine)-*b*-poly-(L-leucine) diblock copolymers, varying both total molecular weight and the relative block lengths. Here we report in more detail on another library where the total molecular weigth was kept constant at 200 amino acid monomers. L-lysine (K) formed the hydrophilic block in all cases, but four different amino acids were used on the hydrophobic end: L-leucine (L), L-isoleucine (I), L-phenylalanine (F) and L-valine (V). In addition, the relative length of the blocks was varied: 95–5%, 90–10%, 80–20% and 70–30%, the hydrophilic lysine segment being the largest in all copolypeptides. The result was a library of 4×4 diblock copolypeptides. Although at first sight 16 may seem a very modest number for high-throughput screening, it should be realized that studying gelation implies that concentration is added as a parameter. We chose to prepare samples at 0.1, 0.3, 1 and 3% by weight in order to span a reasonably wide range of concentrations. As tracer particles we used positively charged amidine functionalized spheres ($a = 0.26\ \mu$m) to prevent aggregation in the presence of positively charged polyelectrolyte blocks. The tracer particles were fluorescently labeled to facilitate microscopy through the bottom of a 96-well plate. Illumination for bright-field microscopy would be a challenge due to sample thickness and plate geometry, whereas fluorescence offers illumination and detection from the same side of the sample. As a result the samples can be protected against evaporation during the experiments by means of plate-sealing film without affecting the optics (Titer-Top, Diversified Biotech, Boston, MA).

Fig. 4 shows the tracer mean-squared displacements for two of the diblock architectures, $K_{190}L_{10}$ and $K_{160}F_{40}$, as a function of concentration. While $K_{190}L_{10}$ remains liquid-like up to 3 wt%, $K_{160}F_{40}$ exhibits more interesting behavior: at 0.1 and 0.3% it is a liquid, at 1% it starts to exhibit viscoelasticity (slope deviates from 1) and at 3% it forms a strong gel. The qualitative rheological classification fulfills the purpose of the gelation study and can easily be made without actually transforming the data into dynamic moduli through Equation 3. An overview of the qualitative rheology of all samples is presented in Table I, where we only distinguish between liquid (L), strong gel (G) and weak viscoelastic gel (WG). There are a few gaps in the data set. One of the block copolypeptides, $K_{140}I_{60}$, did not dissolve in deionized water and could not be measured at all. In some cases, video microscopy could not be performed on the 0.3% samples due to severe aggregation of the tracer particles. Also, a few of the 0.1% samples exhibited a much weaker flocculation at the glass bottom. Depletion flocculation provides a likely explanation. The aggregation was obvious from the movies

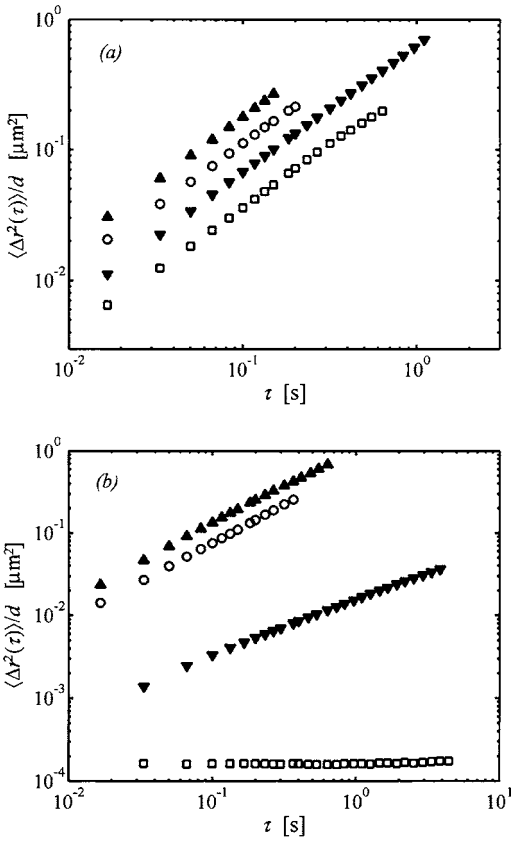

Figure 4 Mean-squared displacement of 0.53 μm spheres (100× objective) in two of the diblock copolypeptides, (a) $K_{190}L_{10}$ and (b) $K_{160}F_{40}$ at different concentrations: (▲) 0.10 wt%, (○) 0.30 wt%, (▼) 1.0 wt% and (□) 3.0 wt%; note the different scales.

TABLE I Overview of the qualitative rheology of all of the diblock copolypeptide solutions; (L) denotes liquid-like behavior, (WG) a weak viscoelastic gel and (G) a strong, elastic gel; × indicates that sample could not be measured with video microrheology. The subscripts in the molecular nomenclature refer to the number of monomers inside the respective blocks; K: lysine, L: leucine, I: isoleucine, F: phenylalanine and V: valine

	0.1%	0.3%	1%	3%
$K_{190}L_{10}$	L	L	L	L
$K_{180}L_{20}$	L	L	L	WG
$K_{160}L_{40}$	L	x	G	G
$K_{140}L_{60}$	L	x	WG	G
$K_{190}I_{10}$	L	x	L	L
$K_{180}I_{20}$	L	x	L	L
$K_{160}I_{40}$	L	L	L	G
$K_{140}I_{60}$	x	x	x	x
$K_{190}F_{10}$	L	L	L	L
$K_{180}F_{20}$	L	L	L	WG
$K_{160}F_{40}$	L	L	WG	G
$K_{140}F_{60}$	L	L	L	G
$K_{190}V_{10}$	L	x	L	L
$K_{180}V_{20}$	L	x	L	L
$K_{160}V_{40}$	L	x	WG	G
$K_{140}L_{60}$	L	L	L	G

and the generation of spurious results was prevented automatically because particle tracking failed.

In spite of the missing data, clear trends can be spotted. Leucine is the most effective gel-former of the hydrophobic amino acids in our study, followed by phenylalanine, valine and isoleucine. Secondly, for all polymers the 70/30 design breaks the trend of increasing strength with hydrophobic content. This is an early warning that we are pushing the limits of solubility and approach the onset of phase separation. Indeed, the 70/30 samples were slightly cloudy, when observed closely, and $K_{140}I_{60}$ did not dissolve at all.

Block copolypeptide hydrogels are an exciting example of the potential of high-throughput rheology when developing new materials and the method will be vital to screen the phase space of possible molecular designs if the complexity of the copolypeptides expands beyond relatively simple diblocks architectures.

5.2. Phase diagram studies

Another area where high-throughput rheology has potential is the screening of phase behavior in multicomponent mixtures. By constructing a sample array where the variable is relative sample composition, one can generate a "rheological phase diagram." Once phase boundaries have been established, samples of interest can be subjected to more labor-intensive characterization techniques to determine the underlying structure in more detail. As proof of concept we have used diffusing-wave spectroscopy to carry out a limited study of the tertiary system consisting of water, sodium dodecyl sulphate (SDS) and NaCl. It is known that the addition of salt changes the properties of the micellar phase due to the growth of elongated wormlike micelles [30]. We have investigated this regime in a small array with SDS concentrations of 15, 20 and 25 wt% in NaCl solutions of respectively 0, 0.1, 0.2 and 0.4 M.

The SDS was dissolved in NaCl solutions with 25% higher concentration than the target value, so that the addition of concentrated suspension of polystyrene tracers yielded the correct composition. Samples were tranferred into a 96 well-plate with optical bottom, volumes of 120 μl resulting in a sample thickness of 3.5 mm. The polystyrene spheres had a diameter of 0.55 μm and volume fraction of 0.9%. The well-plate was protected against evaporation with plate sealing film, that was removed only for the actual DWS measurement.

For a number of the samples the dynamic structure factor $g_1(\tau)$ is presented in Fig. 5 together with the mean-squared displacements that were extracted from the scattering data. The transformation was performed after calibration with polystyrene suspension in deionized water at the same volume fraction as the surfactant solutions.

Both data sets present the same picture: at a fixed SDS concentration, the addition of salt dramatically slows down the particle dynamics, once a threshold value of 0.1 M has been reached. For the highest salt concentration of 0.4 M, the dynamics becomes noticeably more complex, viscoelastic behavior being indicated by the kink in the MSD at long lag times. Similar results

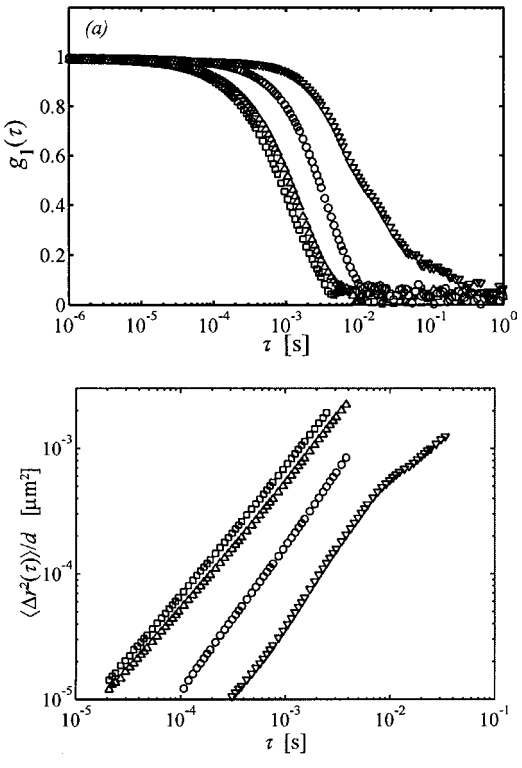

Figure 5 (a) Normalized dynamic structure factors $g_1(t)$ and (b) meansquared displacement for different SDS-water-NaCl mixtures. SDS concentration 20 wt% in (□) 0, (Δ) 0.1, (○) 0.2 and (▽) 0.4 M NaCl. Polystyrene spheres of 550 nm diameter at 0.9 wt%; wavelength $\lambda = 488$ nm and $T = 25\,^{\circ}$C.

are found when the library is scanned along the other axis by increasing the surfactant concentration at constant salinity.

These experiments on a multicomponent surfactant system elucidate how DWS based microrheology can be used to screen libraries of complex fluids with purely compositional variation, thus providing a different range of applications. The big advantage of the DWS is the speed at which the data can be collected due to the inherent ensemble averaging. The correlation measurements described above were performed for 300 s in order to get reliable statistics at the longest times even for the most viscous sample. Further exploration of this application of microrheology remains to be done.

6. Conclusions

Microrheology is an excellent tool for high-throughput screening of the mechanical properties of complex fluids, in particlular the dynamic viscoelastic moduli as a function of frequency. The small sample size and highly automated data analysis enable the rheological characterization of at least 100 samples per day in contrast with 5–10 samples per day on a conventional mechanical rheometer. There is a variety of passive microrheological techniques that all measure the thermal motion of Brownian tracer particles. The statistical analysis of tracer motion yields rheological properties of the embedding medium. Because the Brownian tracer motion is driven by thermal energy $k_B T$, passive microrheoloy is limited to complex fluids that are soft enough for the micrometer sized tracers to undergo detectable motion.

Two implementations of microrheology are particularly suitable for high-throughput screening: video

microscopy and diffusing-wave spectroscopy. Video microscopy requires relatively time-consuming image analysis procedures, but it has the benefit of added spatial resolution since single-particle trajectories are measured. In heterogeneous samples this enables detailed quantitative analysis of the level of heterogeneity. Diffusing-wave spectroscopy, on the other hand, performs ensemble averaging on the fly, so that mean-squared displacements of particles can be measured efficiently by sacrificing spatial resolution.

As in many other high-thoughput techniques, sample library preparation is a critical process. For complex fluids it is not trivial to prepare small volumes of well-defined composition, especially in multi-component mixtures. The need to mix in Brownian tracer particles complicates matters even further. Sample preparation therefore needs to be addressed on a case by case basis. Two examples were presented for which microrheology is a useful high-throughput investigation tool: the gelation behavior of aqueous solutions of block copolypeptide libraries and phase diagrams of multi-component mixtures.

Acknowledgements

We would like to thank Dr. Andrew Nowak (UCSB) for synthesizing the diblock copolypeptide library and Megan Valentine (Harvard) for an introduction into IDL-based particle tracking. We further acknowledge financial support of the Netherlands Organization for Scientific Research (NWO), Unilever and the MRSEC Program of the National Science Foundation (DMR00-80034).

References

1. H. FREUNDLICH and W. SEIFRIZ, *Zeitschrift für Physikalische Chemie* **104** (1922) 233.
2. F. C. MACKINTOSH and C. F. SCHMIDT, *Curr. Opin. Coll. Interf. Sci.* **4** (1999) 300.
3. M. J. SOLOMON and Q. LU, *ibid.* **6** (2001) 430.
4. A. MUKHOPADHYAY and S. GRANICK, *ibid.* **6** (2001) 423.
5. F. ZIEMANN, J. RADLER and E. SACKMANN, *Biophys. J.* **66**(6) (1994) 2210.
6. F. AMBLARD, *et al.*, *Phys. Rev. Lett.* **77**(21) (1996) 4470.
7. A. R. BAUSCH, W. MOLLER and E. SACKMANN, *Biophys. J.* **76**(1) (1999) 573.
8. A. ASHKIN, *Proc. Nat. Acad. Sci. United States of America* **94**(10) (1997) 4853.
9. C. MIO and D. W. M. MARR, *Adv. Mater.* **12**(12) (2000) 917.
10. B. Y. DU, *et al.*, *Langmuir* **17**(11) (2001) 3286.
11. R. E. MAHAFFY, *et al.*, *Phys. Rev. Lett.* **85**(4) (2000) 880.
12. T. G. MASON and D. A. WEITZ, *ibid.* **74**(7) (1995) 1250.
13. A. J. LEVINE and T. C. LUBENSKY, *ibid.* **85**(8) (2000) 1774.
14. B. SCHNURR, *et al.*, *Macromol.* **30**(25) (1997) 7781.
15. T. G. MASON, *et al.*, *Phys. Rev. Lett.* **79**(17) (1997) 3282.
16. T. G. MASON, H. GANG and D. A. WEITZ, *J. Opt. Soc. Amer. a-Optics Image Sci. Vis.* **14**(1) (1997) 139.
17. J. APGAR, *et al.*, *Biophys. J.* **79**(2) (2000) 1095.
18. J. C. CROCKER, *et al.*, *Phys. Rev. Lett.* **85**(4) (2000) 888.
19. M. T. VALENTINE, *et al.*, *Phys. Rev.* E **64** (2001) 061506.
20. A. P. NOWAK, *et al.*, *Nature* **417**(6887) (2002) 424.
21. B. R. DASGUPTA, *et al.*, *Phys. Rev.* E **65** (2002) 051505.
22. T. G. MASON, *Rheol. Acta* **39**(4) (2000) 371.
23. S. G. J. M. KLUIJTMANS, G. H. KOENDERINK and A. P. PHILIPSE, *Phys. Rev.* E **61**(1) (2000) 626.
24. M. KELLER, J. SCHILLING and E. SACKMANN, *Rev. Sci. Instr.* **72**(9) (2001) 3626.
25. J. C. CROCKER and D. G. GRIER, *J. Coll. Interf. Sci.* **179** (1996) 298.
26. M. T. VALENTINE, *et al.*, *Biophys. J.* **80**(1) (2001) 495a.
27. D. A. WEITZ and D. J. PINE, in "Dynamic Light Scattering," edited by W. Brown (Oxford University Press, New York, 1993) p. 652.
28. G. MARET, *Curr. Opin. Coll. Interf. Sci.* **2**(3) (1997) 251.
29. T. J. DEMING, *Nature* **390**(6658) (1997) 386.
30. M. TORNBLOM, U. HENRIKSSON and M. GINLEY, *J. Phys. Chem.* **98**(28) (1994) 7041.